JACS
JOURNAL OF THE AMERICAN CHEMICAL SOCIETY
pubs.acs.org/JACS
Article

Chalcogen Bonding and Hydrophobic Effects Force Molecules into Small Spaces

Faiz-Ur Rahman, Demeter Tzeli, Ioannis D. Petsalakis, Giannoula Theodorakopoulos, Pablo Ballester, Julius Rebek, Jr.,* and Yang Yu*

Cite This: J. Am. Chem. Soc. 2020, 142, 5876−5883
Read Online
ACCESS | Metrics & More | Article Recommendations | Supporting Information

ABSTRACT: Supramolecular capsules are desirable containers for the study of molecular behavior in small spaces and offer applications in transport, catalysis, and material science. We report here the use of chalcogen bonding to form container assemblies that are stable in water. Cavitands **1**−**3** functionalized with 2,1,3-benzoselenadiazole walls were synthesized in good yield from resorcin[4]-arenes. The solid-state single-crystal X-ray structure of **3** showed a dimeric assembly cemented together through multiple Se···N chalcogen bonds. Binding of hydrophobic and amphiphilic guests in D_2O was investigated by ^1H NMR methods and revealed host−guest assemblies of 1:1, 2:1, and 2:2 stoichiometries. Small guests such as *n*-hexane or cyclohexane assembled as 2:2 capsular complexes, larger guests like cyclohexane carboxylic acid or cyclodecane formed 1:1 cavitand complexes, and longer linear guests like *n*-dodecane, cyclohexane carboxylic acid anhydride, and amides created 2:1 capsular complexes. The 2:1 complex of the capsule with cyclohexane carboxylic acid anhydride was stable over 2 weeks, showing that the seam of chalcogen bonds is "waterproof". Selective uptake of cyclohexane over benzene and methyl cyclohexane over toluene was observed in aqueous solution with the capsule. Hydrophobic forces and hydrogen-bonding attractions between guest molecules such as 3-methylbutanoic acid stabilized the assemblies in the presence of the competing effects of water. The high polarizability and modest electronegativity of Se provide a capsule lining complementary to guest C−H bonds. The 2,1,3-benzoselenadiazole walls impart an unusually high magnetic anisotropy to the capsule environment, which is supported by density functional theory calculations.

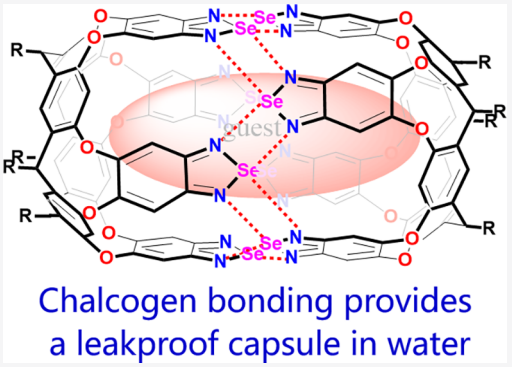

INTRODUCTION

Supramolecular synthetic containers afford confined spaces to affect the behavior of small molecules. The containers isolate molecules from the bulk solution and can stabilize reactive intermediates, even species unknown in solution.[1−3] The supramolecular capsules can be assembled by a variety of forces including metal−ligand interactions developed by Fujita and other groups,[4−9] halogen bonding reported by Diederich,[10−12] hydrogen bonding (HB) explored by our lab,[13−18] and even purely hydrophobic effects introduced by Gibb.[19−22] These supramolecular systems have their advantages and disadvantages, so there is still space for the novel capsules assembled through other attractive forces.

Chalcogen bonding (ChB) involves interactions between σ-holes associated with the electron-deficient chalcogen atoms (S, Se, and Te) and nucleophile sites such as N-donor atoms.[23−25] A number of experimental and theoretical studies detail the nature of the ChB interaction between σ* orbitals and nucleophiles (Figure 1A).[26,27] These interactions are forces of emerging interest in catalysis,[28] transport,[29] and crystal engineering.[27,30−32] Chalcogen bonding in supramolecular chemistry[33,34] is also known, but examples in water[35] are scarce,[8] perhaps because the donors and acceptors of HB in water can compete with ones involved in ChB.

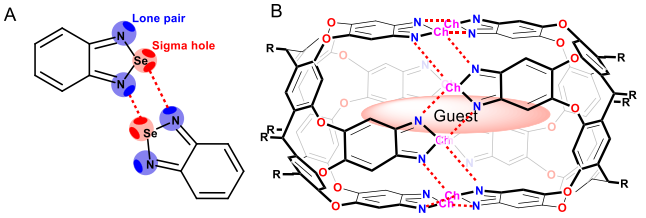

Figure 1. (A) Chalcogen bonding "squares" between Se···N (red dotted lines) in 2,1,3-benzoselenadiazoles. (B) Capsules formed through chalcogen bonding: Ch = S, Te (ref 36); Ch = Se (this work).

Received: February 5, 2020
Published: March 3, 2020

https://dx.doi.org/10.1021/jacs.0c01290
J. Am. Chem. Soc. 2020, 142, 5876−5883

Scheme 1. Synthesis of Water-Soluble Cavitand 1 and Organic-Soluble 2 and 3

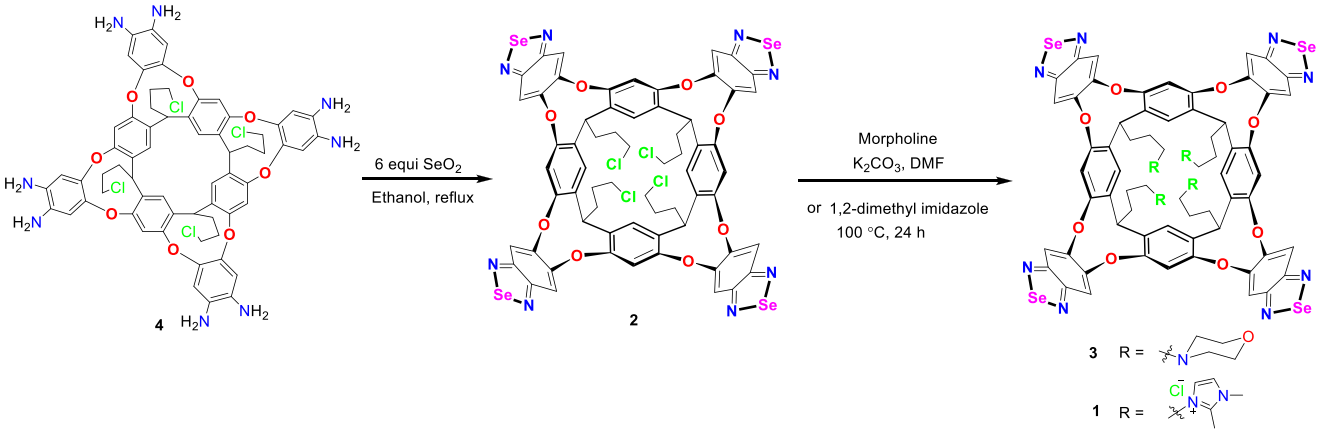

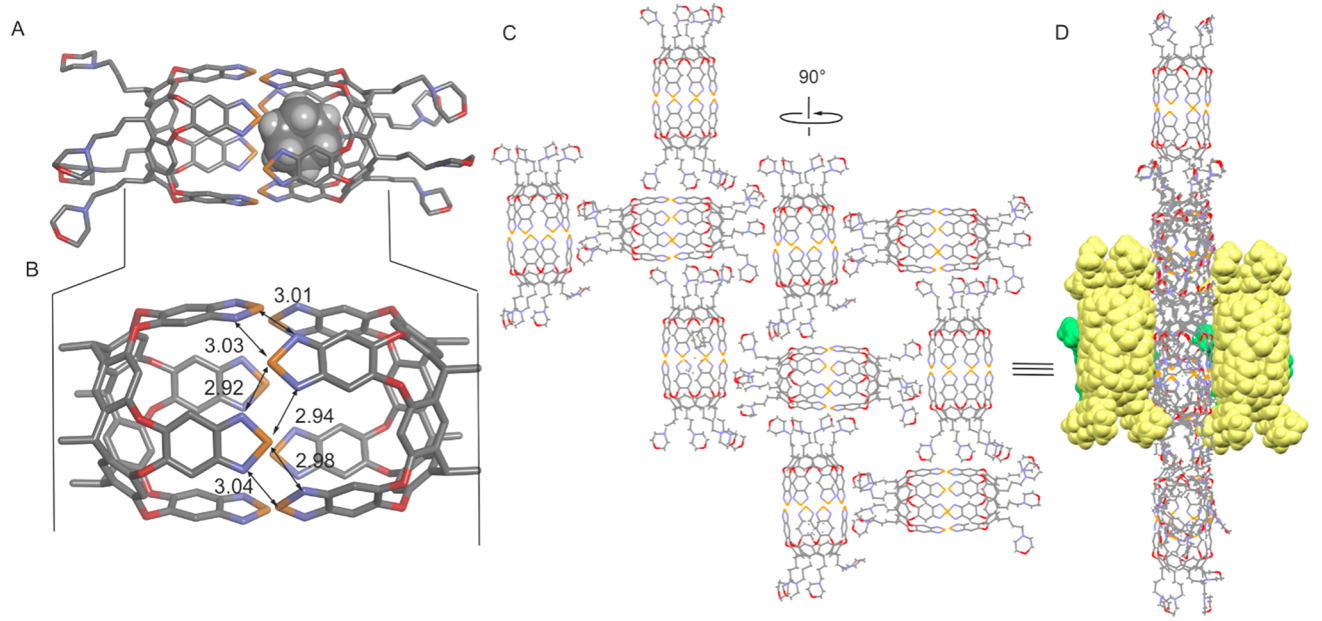

Figure 2. Single-crystal X-ray structure of **3**. (A) Dimeric capsule containing one cyclohexane molecule as a CPK model. (B) Close-up of the circular array of chalcogen bonds stabilizing the capsular dimer with distances in angstroms. (C) Packing of perpendicularly oriented dimeric capsules into rods, which further assemble into layers. (D) Planar layer rotated 90° and sandwiched between two rods (CPK models) of adjacent layers.

Recently, Diederich and coworkers developed capsular complexes by ChB forces in solid-state and organic media.[36] They prepared cavitands with 2,1,3-benzotelluradiazole and 2,1,3-benzothiadiazole walls that assembled to form capsules (Figure 1B, Ch = Te or S). The Te derivative showed strong dimerization in organic media (Figure 1B), but the corresponding S analog was reluctant to do so, probably due to the lower polarizability of S.

Benzoselenadiazoles are also reported to form dimeric structures known as ChB "squares" (Figure 1A).[37−39] The synthesis appeared easier than that of 2,1,3-benzothiadiazoles or 2,1,3-benzotelluradiazoles,[36,40−44] and Se also shows strong ChB interactions with nucleophiles.[41,45] Here we introduce cavitands with such walls in both water-soluble (**1**) and organic soluble versions (**2** and **3**, Scheme 1). The water-soluble cavitand showed 1 + 1 complexes with some guests, but 2 + 2 and 2 + 1 dimeric capsules assembled, depending on the dimensions of the particular guest. The assemblies form in the presence of suitable hydrophobic guests, and they are robust, suggesting that the forces of HB and ChB are more orthogonal than incompatible.

RESULTS AND DISCUSSION

Synthesis. We treated the well-known octaamino cavitand **4**[46] in ethanol with 6 equiv of SeO_2 dissolved in water by stirring and heating the mixture over 5 h (Scheme 1). Cavitand **2** was obtained in excellent isolated yield (93%). The reaction of **2** with morpholine in the presence of K_2CO_3 in warm DMF produced **3**. Similarly, **2** was heated in 1,2-dimethyl imidazole at 100 °C, which gave **1** in 90% yield, which showed good solubility in water. All of these cavitands were isolated in the pure form by merely washing with appropriate organic solvents, then characterized by high-resolution ^1H and ^{13}C NMR spectroscopy and electrospray ionization mass spectrometry (Figures S1−S10)

Solid-State Single-Crystal X-ray Study of the Capsule. Single crystals suitable for X-ray diffraction grew by the slow evaporation of a chloroform−acetone−cyclohexane (1:1:0.1)

https://dx.doi.org/10.1021/jacs.0c01290
J. Am. Chem. Soc. 2020, 142, 5876−5883

Scheme 2. Cartoons of 1 + 1 Host–Guest Cavitand and 2 + 2 and 2 + 1 Host–Guest Capsules

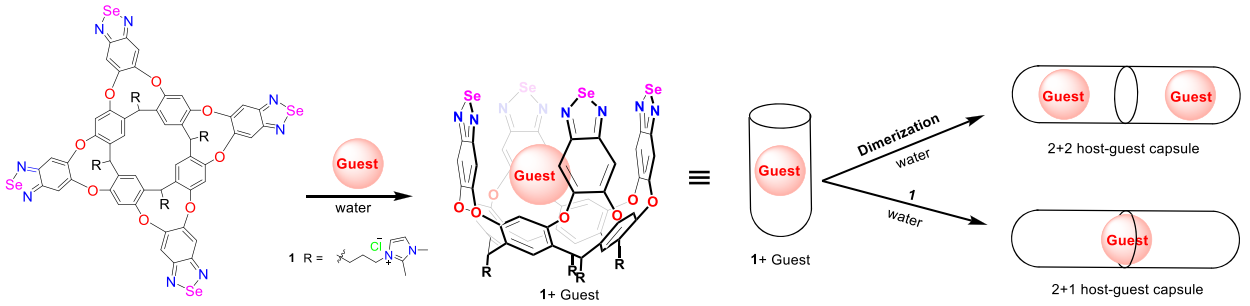

solution mixture of **3**. The small amount of cyclohexane was intended to act as a template to induce the cavitand to adopt the vase conformation by encapsulation. The analysis of the diffracted data revealed that in the solid state, cavitand **3** was present as a capsular dimer (Figure 2A). The interior of the capsule was occupied by partially disordered cyclohexane molecules, making difficult their complete exact location. For this reason, some of the cyclohexane molecules included in the capsule's cavity were "squeezed" during the structure refinement. The diffracted X-ray data also showed the presence of additional solvent molecules in the crystal packing surrounding the capsules, which were also omitted during refinement (Figure 2A and Table S1). In the capsular dimer, two molecules of cavitand **3** are bound by means of a circular array of 16 chalcogen bonds, defining the capsule's equator. The shortest and possibly strongest Se···N interactions define a "square" featuring chalcogen bond lengths of 2.92 and 2.94 Å. Other "squares" displaying comparatively weaker Se···N interactions based on chalcogen bond lengths (3.01 and 3.03 Å or 2.98 and 3.04 Å) are also observed. The circular arrangement of the benzoselenadiazole units demands that the chalcogen bonds deviate from linearity (~162°, N–Se···N angle). This geometric feature is expected to weaken the ChB, yet in solution, the capsule proved to be thermodynamically and kinetically quite stable. The distance between the two Se atoms in the corners of the squares was roughly 3.7 Å (Figure 2B). Remarkably, all benzoselenadiazole units of the cavitand **3** are engaged in four chalcogen bonds. This means that each Se atom makes use of its two sigma-holes to interact with the lone pairs of two N atoms of adjacent benzoselenadiazole units. This interaction mode is substantially different from the one typically observed for the packing of benzoselenadiazole in the solid state, in which the Se atom interacts with only one nitrogen atom of a nearby molecule.

The crystal packing of the capsule, $\mathbf{3}_2$, takes place through its assembly in rods of perpendicularly oriented dimers that are stabilized mainly by CH–π interactions (side-to-tail) (Figure 2C). In turn, the rods pack, forming a planar layer, also through side-to-tail CH–π interactions (Figure 2C). Finally, the assembled planar layers stack one on top of another, establishing side-to-side π–π interactions between parallel oriented capsules and thus producing the 3D structure of the crystal lattice (Figure 2D).

Binding of Guests in D_2O Solution. The solution conformations (vase/kite/dimeric kite or velcrand)[47] of related resorcinarene-derived cavitands are dependent on experimental conditions such as temperature, solvent, and metal ions[48−50] and are readily determined by ^{1}H NMR spectroscopy. The vase form is recognized by its methine proton's characteristic chemical shift at 5.5 ppm, whereas in the kite or velcrand form, it appears below 4 ppm. Cavitand **1** was found in the vase form in DMSO-d_6 or methanol-d_4 and in the velcrand conformation in D_2O (Figures S5, S7, and S8). Hydrophobicity is one of the most important factors that push a guest into the space of such cavitands. On the addition of a suitable hydrophobic guest,[15,51] the kite form of **1** in D_2O was converted to the vase shape, and, depending on the size of the guest, 1 + 1 host–guest cavitand complexes or 2 + 2 and 2 + 1 capsular host–guest complexes were observed (Scheme 2 and Figure 3).

The hydrophobic or amphiphilic guests in **1** include alkanes, cycloalkanes, and branched or cyclic carboxylic acids, and their amides showed binding in **1** in water solution (Scheme 2 and Figure 3). A proclivity for capsule formation with alkanes was observed: Small *n*-alkanes, C5 and C6, bound well in **1** (Figures S11–S24) and formed 2 + 2 host–guest capsular complexes; *n*-heptane did not bind, and C9–C13 formed well-defined 2 + 1 host–guest capsules. The inner space of the capsule could be stabilized by taking up two small molecules, but one *n*-heptane alone was too small, and two were too large to be accommodated. *n*-Octane and *n*-tetradecane were transitional cases and formed a mixture of cavitand and capsule. Longer *n*-alkanes such as C15 or C16 did not bind despite their highest hydrophobicity.[52] No evidence of guest binding or folding with these long alkanes was observed, unlike their behavior in hydrogen-bonded capsules.[53]

Another peculiarity of the capsule derived from **1** compared with hydrogen-bonded capsules previously encountered[13,17] is the magnetic environment within. The terminal methyl ($-CH_3$) groups of each *n*-alkane guest appeared at −3.5 to −3.7 ppm (or $-\Delta\delta$ 4.3 to 4.5). This is similar to their shifts in hydrogen-bonded capsules. These nuclei are in the deepest and narrowest part of the cavity, and the upfield shifts reflect the effects of the resorcinarene platform, which all such cavitands have in common. The methylene signals ($-CH_2-$) in **1** appeared clustered around −2.7 to −2.9 ppm (or $-\Delta\delta$ 3.9 to 4.1), even those *farthest* from the resorcinarene and near the center of the space. This is in contrast with cavitands and capsules with benzimidazolone or pyrazine imide walls, which impart regular and sizable downfield shifts on guest nuclei as they move away from the end of the cavity toward its center. These observations, summarized in Scheme 3, offer challenges to the theory concerning the prediction of anisotropy in cross-conjugated systems. We will discuss below the results of the theoretical data using density functional theory (DFT) calculations of chemical shifts for the capsular assemblies.

Cyclic alkanes were also studied in the capsule of **1** (Figures S25–S30), and again two molecules of smaller size (C5–C7) assembled a capsule. The larger cyclodecane formed neither a 2 + 2 capsule nor a 2 + 1 capsule; instead, it formed a 1 + 1 cavitand, as indicated by the integration of the host methine

https://dx.doi.org/10.1021/jacs.0c01290
J. Am. Chem. Soc. 2020, 142, 5876−5883

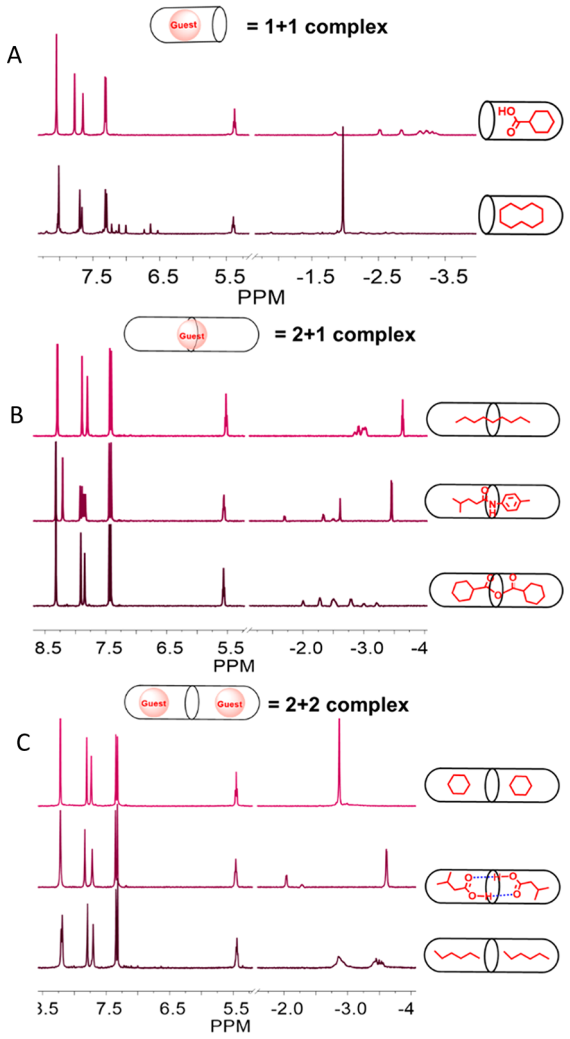

Figure 3. Comparative ^{1}H NMR spectra of **1** in the presence of guests giving different complexes: (A) the 1 + 1 cavitand complexes with cyclodecane or cyclohexane carboxylic acid, (B) the 2 + 1 capsular complexes with anhydrides, amides, or long *n*-alkanes, and (C) 2 + 2 capsular assemblies with short alkanes, acids, or cyclohexane.

Scheme 3. Typical Upfield Chemical Shifts ($-\Delta\delta$) Experienced by Nuclei of Guests Like Octane at Different Depths in Cavitands

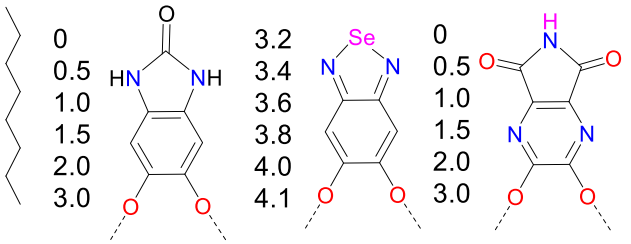

protons and guest protons. Guests from cyclopentane to cyclooctane showed single peaks in their NMR spectra, indicating their fast rotation and translational motion in the space (on the NMR chemical shift time scale). The signal for cyclohexane was observed at −2.87 ppm, indicating an averaged upfield shift of $\Delta\delta$ = −4.27 (Figure S27). An increase in the guest size barely changed the chemical shifts ($\Delta\delta$), denoting the consistent anisotropy throughout the inner space (Figure S25).

Amphiphilic branched-chain or cycloalkyl carboxylic acids showed behavior different from the cyclic alkanes. The smaller and water-soluble isobutyric acid did not bind; that is, it was unable to overcome the stabilization forces of the velcrand. But 3-methyl butanoic acid and cyclopentane carboxylic acid formed 2:2 capsules, suggesting stabilization through an acid−acid hydrogen bond in addition to ChB (Figures S31−S39). The terminal methyl groups of 3-methylbutanoic acid were found deepest in the cavity. To confirm the H bond between the two carboxylic acid groups, we performed the ^{1}H NMR analysis in 10% D_2O in H_2O. This solvent system gave rise to a small signal for COOH protons that persisted even after 1 week (Figures S34 and S35). We observed four downfield-shifted signals for the 2 + 2 capsule of cyclopentane carboxylic acid. The hydrogen of COOH could not be seen in D_2O due to the exchange with D of deuterated water. The cyclopentane carboxylic acid dimer is a rod-like structure of the two molecules that have fast translational motion on the NMR chemical shift time scale in the capsule, as observed by the average shift seen by ^{1}HNMR analysis. Cyclohexane, cycloheptane, and adamantane carboxylic acid gave stable 1 + 1 cavitand inclusion complexes with their C−H groups all inside the cavity (Figures S37−S39). For these larger cycloalkane carboxylic acids, the H-bonded dimer could not be accommodated, so it formed a 1 + 1 cavitand complex by pushing the hydrophobic part deeper in the cavity of **1**. As previously mentioned, the acid−acid hydrogen bond may be a force that stabilizes the capsule. With guests of larger size, this bonding results in a longer assembly of guest molecules that cannot be accommodated, so a 1 + 1 cavitand complex results. The 2 + 2 capsule and acid−acid HB in the case of 3-methylbutanoic acid and cyclopentane carboxylic acid guests can also be deduced from their protons' chemical shifts. In the case of cyclopentane carboxylic acid, the deepest protons' chemical shifts were observed at −2.99 ppm, whereas for cyclohexane carboxylic acid, they were at −3.31 ppm, showing that the bigger sized guest is bound deeper, which is opposite to the previously reported observations for dynamic cavitands.[51,52,54]

To further characterize the capsule, we studied **1** with different medium-sized amides (Figures S40−S46). With 0.5 equiv of the amides, **1** formed a 2 + 1 host−guest capsular complex, as confirmed by the integration ratio of the methine peak of **1** with different protons of the guests. We also confirmed the capsule formation by DOSY analysis in D_2O. The DOSY spectrum for the mixture of cavitand complex (cyclohexane carboxylic acid @ **1**) and capsular complex (cyclohexane carboxylic acid anhydride @ $\mathbf{1}_2$) displays two assemblies with different diffusion constants for the cavitand and capsule complexes (Figures S47−S52).

Theoretical Studies of the Capsular Assemblies. To rationalize the observed ^{1}H NMR chemical shifts, we performed DFT calculations of three capsular complexes corresponding to the three aromatic panels depicted in Scheme 3. The dimeric assemblies studied encapsulated one molecule of *n*-nonane (C_9H_{20}) in an extended conformation. The computational approach involved DFT calculations using two functionals, M062X and PBE0, in conjunction with the 6-31G(d,p) basis set. (See the Supporting Information.) The calculated geometries of the complexes and the computed ^{1}H NMR chemical shifts of the guest are shown in Figure 4. Figure

https://dx.doi.org/10.1021/jacs.0c01290
J. Am. Chem. Soc. 2020, 142, 5876−5883

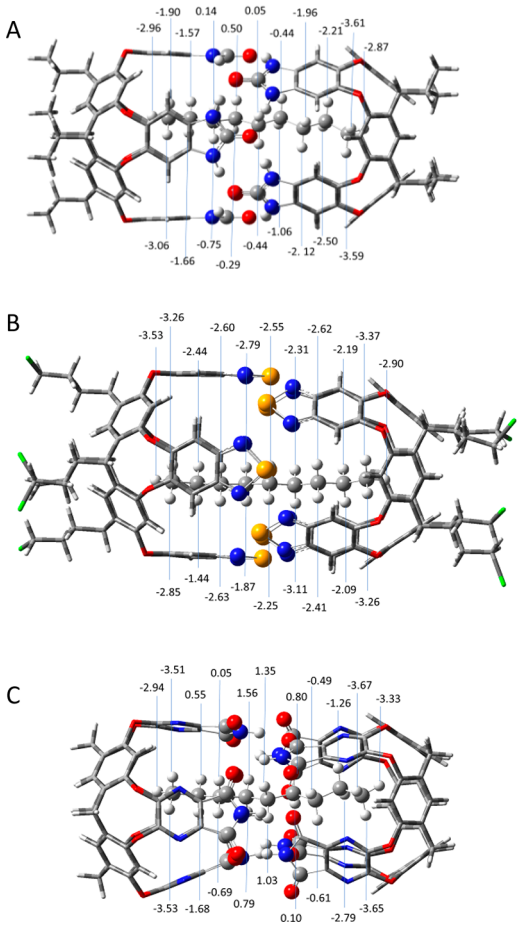

Figure 4. Computed (PBE0/6-31G(d,p)) upfield shifts inside capsules with extended *n*-nonane as a guest: (A) benzimidazolone, (B) benzoselenadiazole, and (C) pyrazine-imide walls.

4A depicts the results of the capsule containing aromatic walls equipped with ureas $(NH)_2C{=}O$ at the rim. Figure 4B shows the results of the calculations on the selenadiazole capsule, and Figure 4C summarizes the results of the capsular assembly displaying aromatic walls with terminal imide functions. The experimentally observed differences in chemical shift values for the encapsulated guest in Figure 4B and the other two examples are nicely reproduced by theory, especially for the hydrogen atoms located at the center of the capsular complex.

The origin of the observed (and calculated) differences in ^{1}H NMR chemical shifts may be attributed to a greater polarizability and enhanced aromaticity of the wall containing the Se atom. Its increased magnetic anisotropy, in comparison with the capsules featuring urea and imide functions, is detailed in the Supporting Information. (See Table 1.) The increase in the isotropic (anisotropic) polarizability in the Se-capsule (Figure 4B) compared with Figure 4A is ~22 (42)%, and compared with **4C**, it is 46 (141)%. (These capsules correspond to the first and third panels of Scheme 3.)

Table 1. Percent Increase in Dipole Electric Field Isotropic and Anisotropic Polarizabilities of 4B Se-capsule with Respect to 4A and 4C (See Also Scheme 3)

	4A		4C	
	caps	caps + guest	caps	caps + guest
iso	22	22	46	45
aniso	42	41	141	125

Binding Selectivity of 1. Cyclohexane and methyl cyclohexane are prepared on an industrial scale by the hydrogenation of benzene and toluene, respectively. Selective sequestration of mixtures of benzene−cyclohexane or toluene−methyl cyclohexane is desirable in the production of these compounds.[55−59] We found selective encapsulation of cyclohexane over benzene and methyl cyclohexane over toluene using **1** as a host. In the presence of benzene and cyclohexane, **1** encapsulated two cyclohexane molecules and formed the 2 + 2 capsule (Scheme 4 and Figures S53−S60). Similarly, **1** showed excellent selectivity for methyl cyclohexane over toluene, again forming a 2 + 2 capsular assembly (Scheme 4 and Figures S61−S68).

Scheme 4. Schematic Representation of the Selective Uptake of Two Molecules of Cyclohexane over Benzene and Two Molecules of Methyl Cyclohexane over Toluene in Capsular Dimer of 1

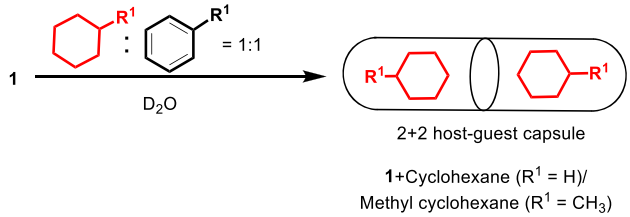

Miscellaneous Guest Binding. The action of **1** on 4,4′-dimethyl biphenyl, 1-halooctanes (chloro, bromo, and iodo), and 1,8-dibromooctane led to the assembly of the corresponding 2 + 1 capsular complexes by encapsulation of one molecule of the guests (Figure 5 and Figures S69−S74). In the case of

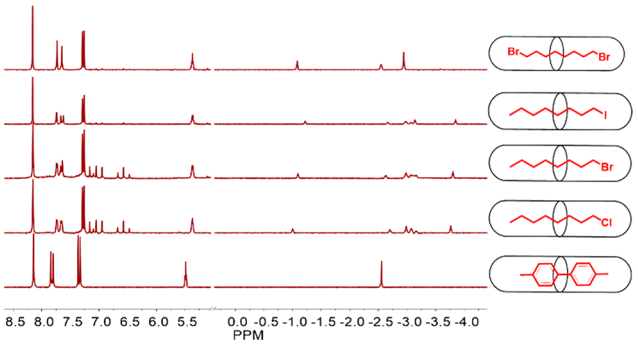

Figure 5. Partial ^{1}H NMR spectra and cartoons of the capsule complexes.

4,4′-dimethylbiphenyl, the guest's six methyl protons were observed upfield-shifted at −2.55 ppm, and its two aromatic protons were observed at 3.03 and 3.30 ppm, again indicative of large upfield shifts throughout the capsule (Figure 5 and Figures S69 and S70). For 1-halooctanes, the terminal methyl protons' chemical shifts were easily recognized for chloro-, bromo-, and iodooctane at −3.76, −3.80, and −3.85 ppm, respectively. For the $-CH_2-X$ groups of chloro-, bromo-, and iodooctane, the protons' chemical shifts were observed at −1.0, −1.09, and −1.23 ppm, respectively. The remaining six methylenes of these guests were clustered around −3.00 ppm, showing that they occupied the middle region of the

https://dx.doi.org/10.1021/jacs.0c01290
J. Am. Chem. Soc. 2020, 142, 5876−5883

capsule (Figure 5 and Figures S71−S73). 1,8-Dibromooctane also formed a 2 + 1 host−guest capsule showing a linear conformation in the space with the two terminal bromides at the ends of the capsule. The chemical shift for $-CH_2-Br$ (four protons) was observed at −1.08 ppm (the largest $\Delta\delta$), whereas the next methylenes (four protons) were observed at −2.55 ppm. The remaining four methylene signals were clustered at −2.94 ppm (Figure 5 and Figure S74). In the spectra of 1-chlorooctane and 1-bromooctane, we also saw a small amount of velcrand (free cavitand), showing the reversibility of the host−guest complex that may be due to the higher polarity and the greater water solubility of these guests.

CONCLUSIONS

We described chalcogen-bonded supramolecular capsules in water using a deep cavitand with 2,1,3-benzoselenadiazole walls. Single-crystal X-ray structure analysis in the solid state and high-resolution NMR and DOSY spectroscopy in solution characterized the host−guest encapsulation complexes with hydrophobic or amphiphilic guest molecules. For cavitand **1** dissolved in D_2O, we observed 1 + 1 host−guest cavitand complexes and 2 + 1 and 2 + 2 host−guest capsular complexes. This cavitand showed selectivities for cyclohexane over benzene and methyl cyclohexane over toluene that may lead to applications for selective sensing and energy-efficient separations through solvent−solvent extraction processes. Both experimental data and theoretical calculations show that the chalcogen-bonded capsule features enhanced magnetic anisotropy. This study confirms that ChB persists well in water, in competition with the forces of HB.

ASSOCIATED CONTENT

Supporting Information

The Supporting Information is available free of charge at https://pubs.acs.org/doi/10.1021/jacs.0c01290.

Single-crystal X-ray data (CCDC no. 1967953) (CIF)

Related procedures, general experimental, synthetic procedures, and original ^1H NMR and MS spectra (PDF)

AUTHOR INFORMATION

Corresponding Authors

Julius Rebek, Jr. − *Center for Supramolecular Chemistry & Catalysis and Department of Chemistry, College of Science, Shanghai University, Shanghai 200444, China; Skaggs Institute for Chemical Biology and Department of Chemistry, The Scripps Research Institute, La Jolla, California 92037, United States;* orcid.org/0000-0002-2768-0945; Email: jrebek@scripps.edu

Yang Yu − *Center for Supramolecular Chemistry & Catalysis and Department of Chemistry, College of Science, Shanghai University, Shanghai 200444, China;* orcid.org/0000-0001-5698-3534; Email: yangyu2017@shu.edu.cn

Authors

Faiz-Ur Rahman − *Center for Supramolecular Chemistry & Catalysis and Department of Chemistry, College of Science, Shanghai University, Shanghai 200444, China;* orcid.org/0000-0002-4006-8881

Demeter Tzeli − *Theoretical and Physical Chemistry Institute, The National Hellenic Research Foundation, Athens 11635, Greece; Laboratory of Physical Chemistry, Department of Chemistry, National and Kapodistrian University of Athens, Athens 157 71, Greece;* orcid.org/0000-0003-0899-7282

Ioannis D. Petsalakis − *Theoretical and Physical Chemistry Institute, The National Hellenic Research Foundation, Athens 11635, Greece*

Giannoula Theodorakopoulos − *Theoretical and Physical Chemistry Institute, The National Hellenic Research Foundation, Athens 11635, Greece*

Pablo Ballester − *Institute of Chemical Research of Catalonia (ICIQ), 43007 Tarragona, Spain; Catalan Institution for Research and Advanced Studies (ICREA), 08010 Barcelona, Spain;* orcid.org/0000-0001-8377-6610

Complete contact information is available at: https://pubs.acs.org/10.1021/jacs.0c01290

Notes

The authors declare no competing financial interest.

ACKNOWLEDGMENTS

This work was supported by the National Natural Science Foundation of China (grant no. 21801164), the U.S. National Science Foundation (CHE 1801153), and Shanghai University (N.13-G210-19-230), Shanghai, China. Y.Y. thanks the Program for Professor of Special Appointment (Dongfang Scholarship) of the Shanghai Education Committee.

ABBREVIATIONS

HB, hydrogen bonding; ChB, chalcogen bonding

REFERENCES

(1) Yoshizawa, M.; Klosterman, J. K.; Fujita, M. Functional molecular flasks: new properties and reactions within discrete, self-assembled hosts. *Angew. Chem., Int. Ed.* **2009**, *48* (19), 3418−38.

(2) Zhang, Q.; Catti, L.; Tiefenbacher, K. Catalysis inside the Hexameric Resorcinarene Capsule. *Acc. Chem. Res.* **2018**, *51* (9), 2107−2114.

(3) Zhu, Y.; Rebek, J., Jr; Yu, Y. Cyclizations catalyzed inside a hexameric resorcinarene capsule. *Chem. Commun. (Cambridge, U. K.)* **2019**, *55* (25), 3573−3577.

(4) Hatakeyama, Y.; Sawada, T.; Kawano, M.; Fujita, M. Conformational preferences of short peptide fragments. *Angew. Chem., Int. Ed.* **2009**, *48* (46), 8695−8.

(5) Kawano, M.; Kobayashi, Y.; Ozeki, T.; Fujita, M. Direct crystallographic observation of a coordinatively unsaturated transition-metal complex in situ generated within a self-assembled cage. *J. Am. Chem. Soc.* **2006**, *128* (20), 6558−9.

(6) Pluth, M. D.; Bergman, R. G.; Raymond, K. N. Proton-mediated chemistry and catalysis in a self-assembled supramolecular host. *Acc. Chem. Res.* **2009**, *42* (10), 1650−9.

(7) Piper, J. R.; Cletheroe, L.; Taylor, C. G.; Metherell, A. J.; Weinstein, J. A.; Sazanovich, I. V.; Ward, M. D. Photoinduced energy- and electron-transfer from a photoactive coordination cage to bound guests. *Chem. Commun. (Cambridge, U. K.)* **2017**, *53* (2), 408−411.

(8) Spicer, R. L.; Stergiou, A. D.; Young, T. A.; Duarte, F.; Symes, M. D.; Lusby, P. J. Host-Guest-Induced Electron Transfer Triggers Radical-Cation Catalysis. *J. Am. Chem. Soc.* **2020**, *142* (5), 2134−2139.

(9) Cai, L. X.; Li, S. C.; Yan, D. N.; Zhou, L. P.; Guo, F.; Sun, Q. F. Water-Soluble Redox-Active Cage Hosting Polyoxometalates for Selective Desulfurization Catalysis. *J. Am. Chem. Soc.* **2018**, *140* (14), 4869−4876.

(10) Gropp, C.; Quigley, B. L.; Diederich, F. Molecular Recognition with Resorcin[4]arene Cavitands: Switching, Halogen-Bonded Capsules, and Enantioselective Complexation. *J. Am. Chem. Soc.* **2018**, *140* (8), 2705−2717.

(11) Dumele, O.; Trapp, N.; Diederich, F. Halogen bonding molecular capsules. *Angew. Chem., Int. Ed.* **2015**, *54* (42), 12339−44.
(12) Dumele, O.; Schreib, B.; Warzok, U.; Trapp, N.; Schalley, C. A.; Diederich, F. Halogen-Bonded Supramolecular Capsules in the Solid State, in Solution, and in the Gas Phase. *Angew. Chem., Int. Ed.* **2017**, *56* (4), 1152−1157.
(13) Tiefenbacher, K.; Zhang, K.-d.; Ajami, D.; Rebek, J. Robust hydrogen-bonded capsules with stability in competitive media. *J. Phys. Org. Chem.* **2015**, *28* (3), 187−190.
(14) Gavette, J. V.; Zhang, K. D.; Ajami, D.; Rebek, J., Jr Folded alkyl chains in water-soluble capsules and cavitands. *Org. Biomol. Chem.* **2014**, *12* (34), 6561−3.
(15) Zhang, K. D.; Ajami, D.; Rebek, J. Hydrogen-bonded capsules in water. *J. Am. Chem. Soc.* **2013**, *135* (48), 18064−6.
(16) Sarwar, M. G.; Ajami, D.; Theodorakopoulos, G.; Petsalakis, I. D.; Rebek, J., Jr Amplified halogen bonding in a small space. *J. Am. Chem. Soc.* **2013**, *135* (37), 13672−5.
(17) Scarso, A.; Trembleau, L.; Rebek, J. Encapsulation induces helical folding of alkanes. *Angew. Chem.* **2003**, *115* (44), 5657−5660.
(18) Heinz, T.; Rudkevich, D. M.; Rebek, J. Pairwise selection of guests in a cylindrical molecular capsule of nanometre dimensions. *Nature* **1998**, *394* (6695), 764−766.
(19) Wang, K.; Cai, X.; Yao, W.; Tang, D.; Kataria, R.; Ashbaugh, H. S.; Byers, L. D.; Gibb, B. C. Electrostatic Control of Macrocyclization Reactions within Nanospaces. *J. Am. Chem. Soc.* **2019**, *141* (16), 6740−6747.
(20) Murray, J.; Kim, K.; Ogoshi, T.; Yao, W.; Gibb, B. C. The aqueous supramolecular chemistry of cucurbit[n]urils, pillar[n]arenes and deep-cavity cavitands. *Chem. Soc. Rev.* **2017**, *46* (9), 2479−2496.
(21) Gibb, C. L.; Gibb, B. C. Templated assembly of water-soluble nano-capsules: inter-phase sequestration, storage, and separation of hydrocarbon gases. *J. Am. Chem. Soc.* **2006**, *128* (51), 16498−9.
(22) Gibb, C. L.; Gibb, B. C. Well-defined, organic nanoenvironments in water: the hydrophobic effect drives a capsular assembly. *J. Am. Chem. Soc.* **2004**, *126* (37), 11408−9.
(23) Murray, J. S.; Lane, P.; Politzer, P. Expansion of the sigma-hole concept. *J. Mol. Model.* **2009**, *15* (6), 723−9.
(24) Pascoe, D. J.; Ling, K. B.; Cockroft, S. L. The origin of chalcogen-bonding interactions. *J. Am. Chem. Soc.* **2017**, *139* (42), 15160−15167.
(25) Cozzolino, A. F.; Elder, P. J. W.; Vargas-Baca, I. A survey of tellurium-centered secondary-bonding supramolecular synthons. *Coord. Chem. Rev.* **2011**, *255* (11−12), 1426−1438.
(26) Cozzolino, A. F.; Vargas-Baca, I.; Mansour, S.; Mahmoudkhani, A. H. The nature of the supramolecular association of 1,2,5-chalcogenadiazoles. *J. Am. Chem. Soc.* **2005**, *127* (9), 3184−90.
(27) Gleiter, R.; Haberhauer, G.; Werz, D. B.; Rominger, F.; Bleiholder, C. From Noncovalent Chalcogen-Chalcogen Interactions to Supramolecular Aggregates: Experiments and Calculations. *Chem. Rev.* **2018**, *118* (4), 2010−2041.
(28) Benz, S.; Lopez-Andarias, J.; Mareda, J.; Sakai, N.; Matile, S. Catalysis with chalcogen bonds. *Angew. Chem., Int. Ed.* **2017**, *56* (3), 812−815.
(29) Borissov, A.; Marques, I.; Lim, J. Y. C.; Felix, V.; Smith, M. D.; Beer, P. D. Anion recognition in water by charge-neutral halogen and chalcogen bonding foldamer receptors. *J. Am. Chem. Soc.* **2019**, *141* (9), 4119−4129.
(30) Chen, L.; Xiang, J.; Zhao, Y.; Yan, Q. Reversible self-assembly of supramolecular vesicles and nanofibers driven by chalcogen-bonding interactions. *J. Am. Chem. Soc.* **2018**, *140* (23), 7079−7082.
(31) Scilabra, P.; Terraneo, G.; Resnati, G. The chalcogen bond in crystalline solids: A world parallel to halogen bond. *Acc. Chem. Res.* **2019**, *52* (5), 1313−1324.
(32) Werz, D. B.; Gleiter, R.; Rominger, F. Nanotube formation favored by chalcogen-chalcogen interactions. *J. Am. Chem. Soc.* **2002**, *124* (36), 10638−9.
(33) Lim, J. Y.; Marques, I.; Thompson, A. L.; Christensen, K. E.; Felix, V.; Beer, P. D. Chalcogen bonding macrocycles and [2]rotaxanes for anion recognition. *J. Am. Chem. Soc.* **2017**, *139* (8), 3122−3133.
(34) Cozzolino, A. F.; Dimopoulos-Italiano, G.; Lee, L. M.; Vargas-Baca, I. Chalcogen-nitrogen secondary bonding interactions in the gas phase - spectrometric detection of ionized benzo-2,1,3-telluradiazole dimers. *Eur. J. Inorg. Chem.* **2013**, *2013* (15), 2751−2756.
(35) Fick, R. J.; Kroner, G. M.; Nepal, B.; Magnani, R.; Horowitz, S.; Houtz, R. L.; Scheiner, S.; Trievel, R. C. Sulfur-oxygen chalcogen bonding mediates AdoMet recognition in the lysine methyltransferase SET7/9. *ACS Chem. Biol.* **2016**, *11* (3), 748−54.
(36) Riwar, L. J.; Trapp, N.; Root, K.; Zenobi, R.; Diederich, F. Supramolecular capsules: strong versus weak chalcogen bonding. *Angew. Chem., Int. Ed.* **2018**, *57* (52), 17259−17264.
(37) Pollice, R.; Chen, P. A Universal quantitative descriptor of the dispersion interaction potential. *Angew. Chem., Int. Ed.* **2019**, *58* (29), 9758−9769.
(38) Lenardão, E. J.; Santi, C.; Sancineto, L. Nonbonded Interaction: The Chalcogen Bond. In *New Frontiers in Organoselenium Compounds*; Springer: Cham, Switzerland, 2018.
(39) Lee, J.; Lee, L. M.; Arnott, Z.; Jenkins, H.; Britten, J. F.; Vargas-Baca, I. Sigma-hole interactions in the molecular and crystal structures of N-boryl benzo-2,1,3-selenadiazoles. *New J. Chem.* **2018**, *42* (13), 10555−10562.
(40) Eichstaedt, K.; Wasilewska, A.; Wicher, B.; Gdaniec, M.; Połoński, T. Supramolecular synthesis based on a combination of Se···N secondary bonding interactions with hydrogen and halogen bonds. *Cryst. Growth Des.* **2016**, *16* (3), 1282−1293.
(41) Garrett, G. E.; Gibson, G. L.; Straus, R. N.; Seferos, D. S.; Taylor, M. S. Chalcogen bonding in solution: interactions of benzotelluradiazoles with anionic and uncharged Lewis bases. *J. Am. Chem. Soc.* **2015**, *137* (12), 4126−33.
(42) Kovtonyuk, V. N.; Makarov, A. Y.; Shakirov, M. M.; Zibarev, A. V. A polyfluoroaromatic tellurium−nitrogen compound: synthesis and properties of 4,5,6,7-tetrafluoro-2λ4δ2,1,3-benzotelluradiazole. *Chem. Commun.* **1996**, No. 16, 1991−1992.
(43) He, L.; Ji, S.; Lai, H.; Chen, T. Selenadiazole derivatives as theranostic agents for simultaneous cancer chemo-/radiotherapy by targeting thioredoxin reductase. *J. Mater. Chem. B* **2015**, *3* (42), 8383−8393.
(44) Khuhawar, M. Y.; Bozdar, R. B.; Babar, M. A. High-performance liquid chromatographic determination of selenium in coal after derivatization to 2,1,3-benzoselenadiazoles. *Analyst* **1992**, *117* (11), 1725−1727.
(45) Lindner, B. D.; Coombs, B. A.; Schaffroth, M.; Engelhart, J. U.; Tverskoy, O.; Rominger, F.; Hamburger, M.; Bunz, U. H. From thia- to selenadiazoles: changing interaction priority. *Org. Lett.* **2013**, *15* (3), 666−9.
(46) (a) Mosca, S.; Yu, Y.; Rebek, J., Jr Preparative scale and convenient synthesis of a water-soluble, deep cavitand. *Nat. Protoc.* **2016**, *11* (8), 1371−87. (b) Yu, Y.; Rebek, J., Jr Reactions of Folded Molecules in Water. *Acc. Chem. Res.* **2018**, *51* (12), 3031−3040.
(47) Cram, D. J.; Choi, H. J.; Bryant, J. A.; Knobler, C. B. Solvophobic and entropic driving forces for forming velcraplexes, which are 4-fold, lock-key dimers in organic media. *J. Am. Chem. Soc.* **1992**, *114* (20), 7748−7765.
(48) Skinner, P. J.; Cheetham, A. G.; Beeby, A.; Gramlich, V.; Diederich, F. Conformational switching of resorcin[4]arene cavitands by protonation, preliminary communication. *Helv. Chim. Acta* **2001**, *84* (7), 2146−2153.
(49) Azov, V. A.; Jaun, B.; Diederich, F. NMR investigations into the vase-Kite conformational switching of resorcin[4]arene cavitands. *Helv. Chim. Acta* **2004**, *87* (2), 449−462.
(50) Frei, M.; Marotti, F.; Diederich, F. Zn(II)-induced conformational control of amphiphilic cavitands in langmuir monolayers. *Chem. Commun.* **2004**, No. 12, 1362−3.
(51) Rahman, F.-U.; Feng, H.-N.; Yu, Y. A new water-soluble cavitand with deeper guest binding properties. *Org. Chem. Front.* **2019**, *6* (7), 998−1001.

https://dx.doi.org/10.1021/jacs.0c01290
J. Am. Chem. Soc. 2020, 142, 5876−5883

(52) Rahman, F. U.; Li, Y. S.; Petsalakis, I. D.; Theodorakopoulos, G.; Rebek, J., Jr; Yu, Y. Recognition with metallo cavitands. *Proc. Natl. Acad. Sci. U. S. A.* **2019**, *116* (36), 17648−17653.
(53) Zhang, K. D.; Ajami, D.; Gavette, J. V.; Rebek, J., Jr Alkyl groups fold to fit within a water-soluble cavitand. *J. Am. Chem. Soc.* **2014**, *136* (14), 5264−6.
(54) Feng, H.-N.; Petroselli, M.; Zhang, X.-H.; Rebek, J., Jr.; Yu, Y. Cavitands: capture of cycloalkyl derivatives and 2-methylisoborneol (2-MIB) in water. *Supramol. Chem.* **2019**, *31* (3), 108−113.
(55) Jie, K.; Zhou, Y.; Li, E.; Zhao, R.; Huang, F. Separation of aromatics/cyclic aliphatics by nonporous adaptive pillararene crystals. *Angew. Chem., Int. Ed.* **2018**, *57* (39), 12845−12849.
(56) Wan, Y.; Chen, C.; Xiao, W.; Jian, L.; Zhang, N. Ni/MIL-120: An efficient metal−organic framework catalyst for hydrogenation of benzene to cyclohexane. *Micropor. Mesopor. Mater.* **2013**, *171*, 9−13.
(57) Mukherjee, S.; Desai, A. V.; Ghosh, S. K. Potential of metal−organic frameworks for adsorptive separation of industrially and environmentally relevant liquid mixtures. *Coord. Chem. Rev.* **2018**, *367*, 82−126.
(58) Shiau, L.-D.; Yu, C.-C. Separation of the benzene/cyclohexane mixture by stripping crystallization. *Sep. Purif. Technol.* **2009**, *66* (2), 422−426.
(59) Kuila, S. B.; Ray, S. K. Separation of benzene−cyclohexane mixtures by filled blend membranes of carboxymethyl cellulose and sodium alginate. *Sep. Purif. Technol.* **2014**, *123*, 45−52.

https://dx.doi.org/10.1021/jacs.0c01290
J. Am. Chem. Soc. 2020, 142, 5876−5883